

# Cooperation between the Two Heads of Smooth Muscle Myosin Is Essential for Full Activation of the Motor Function by Phosphorylation

Rong-Na Ma,<sup>†,‡</sup> Katsuhide Mabuchi,<sup>§</sup> Jing Li,<sup>‡</sup> Zekuan Lu,<sup>‡</sup> Chih-Lueh Albert Wang,<sup>||</sup> and Xiang-dong Li<sup>\*,‡</sup>

<sup>†</sup>School of Life Sciences, University of Science and Technology of China, Hefei, Anhui 230027, China

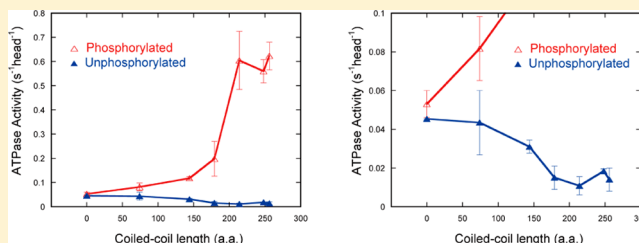
<sup>‡</sup>Group of cell motility and muscle contraction, National Laboratory of Integrated Management of Insect Pests and Rodents, Institute of Zoology, Chinese Academy of Sciences, Beijing 100101, China

<sup>§</sup>Boston Biomedical Research Institute, Watertown, Massachusetts 02472, United States

<sup>||</sup>Department of Physiology and Biophysics, Boston University School of Medicine, Boston, Massachusetts 02118, United States

## Supporting Information

**ABSTRACT:** The motor function of smooth muscle myosin (SmM) is regulated by phosphorylation of the regulatory light chain (RLC) bound to the neck region of the SmM heavy chain. It is generally accepted that unphosphorylated RLC induces interactions between the two heads and between the head and the tail, thus inhibiting the motor activity of SmM, whereas phosphorylation of RLC interrupts those interactions, thus reversing the inhibition and restoring the motor activity to the maximal value. One assumption of this model is that single-headed SmM is fully active regardless of phosphorylation. To re-evaluate this model, we produced a number of SmM constructs with coiled coils of various lengths and examined their structure and regulation. With these constructs we identified the segment in the coiled-coil key for the formation of a stable double-headed structure. In agreement with the current model, we found that the actin-activated ATPase activity of unphosphorylated SmM increased with shortening of the coiled-coil. However, contrary to the current model, we found that the actin-activated ATPase activity of phosphorylated SmM decreased with shortening coiled-coil and only the stable double-headed SmM was fully activated by phosphorylation. These results indicate that single-headed SmM is neither fully active nor fully inhibited. Based on our findings, we propose that cooperation between the two heads is essential, not only for the inhibition of unphosphorylated SmM, but also for the activation of phosphorylated SmM.



Smooth muscle myosin (SmM) is a hexameric molecule composed of two heavy chains, two essential light chains (ELC), and two regulatory light chains (RLC). The motor activity of SmM is activated by phosphorylation of serine 19 on the RLC.<sup>1,2</sup> The unphosphorylated form of SmM is inactive, i.e., it has low actin-activated ATPase activity and is incapable to move actin filaments *in vitro*, whereas the phosphorylated form is active in both respects.

SmM shares the same basic structural features of all myosin II molecules. Each molecule has two globular head domains that are the sites of enzymatic activity (i.e., force generation). Within each head the two myosin light chains bind to an extended  $\alpha$ -helix of the heavy chain that functions as a “lever arm” amplifying small movements generated within the myosin head. Beyond the light chain domain, the myosin molecule dimerizes by virtue of an  $\alpha$ -helical coiled-coil.

The significance of a double-headed structure for the regulation of myosin II has been studied extensively in various myosins. It has been shown that the maximal actin-activated rates of ATP hydrolysis by the skeletal muscle myosin subfragment 1 (S1) and by HMM are approximately the

same,<sup>3</sup> suggesting a relatively independent functional role for each of the two heads of this type of myosin. In contrast, for *Dictyostelium discoideum* myosin II, the phosphorylated single-headed myosin and S1 have much lower actin-activated ATPase activity than phosphorylated double-headed myosin,<sup>4–6</sup> suggesting that cooperativity between the two heads is required for maximum activity of *Dictyostelium* myosin II.

A double-headed structure is required for the regulation of SmM by phosphorylation of the RLC. It is generally accepted that RLC of SmM being in the unphosphorylated state induces interactions between the two heads and between the head and the tail, thus inhibiting the motor activity, whereas phosphorylation of the RLC interrupts those interactions, thus reversing the inhibition and restoring the motor activity to the maximal value.<sup>2,7</sup> According to this model, the default state of the SmM motor is active. One assumption for this model is that single-

Received: May 2, 2013

Revised: August 13, 2013

Published: August 15, 2013



headed SmM, such as S1, is fully active regardless of phosphorylation. However, previous studies have shown that S1 produced by limited protease treatment is only partially active.<sup>8–11</sup> Since proteolytically prepared S1 could have internal nicks in the motor domain, which might alter the activity of the motor domain, it was proposed that the lower-than-expected activity of these S1 preparations was due to these undesired nicks.<sup>12</sup> Indeed, Sata et al. reported that recombinant S1 expressed in insect cells having no nicks has the same actin-activated ATPase activity, regardless of the state of phosphorylation, as the phosphorylated HMM.<sup>13</sup> On the other hand, Konishi et al. found that the actin-activated ATPase activity of recombinant S1 is substantially lower than that of phosphorylated HMM.<sup>14</sup> Thus, whether S1 is fully active remains controversial, and the effect of a double-headed structure on SmM activation by phosphorylation has yet to be adequately addressed.

In the present study, we investigated the role of a double-headed structure on SmM regulation by examining a series of SmM constructs with different lengths of coiled-coil. We found that shortening of the coiled-coil of SmM destabilized the double-headed structure and decreased the actin-activated ATPase activity of phosphorylated SmM. Based on our findings, we propose that a stable double-headed structure is essential for the full activation of SmM by phosphorylation.

## EXPERIMENTAL PROCEDURES

**Materials.** Restriction enzymes and modifying enzymes were purchased from New England Biolabs. *S. aureus* V8 protease (SAP-V8) and papain were purchased from Sigma-Aldrich and Worthington Biochemicals, respectively. Rabbit actin and recombinant human calmodulin (CaM) were prepared as described.<sup>15</sup>

**SmM Truncation Constructs.** Chicken SmM heavy chain was subcloned into a baculovirus transfer pFastHTc (a modified baculovirus transfer vector pFastHTc, Life Technologies) using SpeI and XhoI sites. Truncated SmM was produced by introducing stop codons at various sites in SmM (Figure 1). To facilitate purification, all SmM truncations contain a common N-terminal tag (MSYYH HHHHH DYKDD DDKNI PTEN LYFQG AMGIR NSKAY VDELT S; underline indicates FLAG-tag). The recombinant baculovirus was produced by using a Bac-To-Bac kit (Life Technologies). The recombinant baculoviruses expressing ELC or RLC were prepared as described.<sup>13</sup>

**Expression and Purification of SmM Truncated Constructs.** To express SmM constructs, Sf9 cells were coinfecting with three recombinant baculoviruses expressing the truncated SmM heavy chain, ELC, and RLC, respectively. The expressed proteins were purified by Anti-FLAG M2 agarose affinity chromatography (Sigma-Aldrich) in a procedure as described for unconventional myosin-5a,<sup>16</sup> except that the purified SmM constructs were dialyzed against 50 mM KCl, 0.1 mM EGTA, 10 mM Tris-HCl pH 7.5, 1 mM DTT, and 10% glycerol before being aliquoted, quick-frozen in liquid nitrogen, and stored at  $-80^{\circ}\text{C}$ . All experiments were done with the unphosphorylated material unless indicated otherwise.

**Size-Exclusion Chromatography of SmM Constructs.** A mixture of Sm-849, Sm-923, Sm-993, Sm-1028, and Sm-1063 (200  $\mu\text{L}$ ) was applied to a Superdex G200 size-exclusion column (10  $\times$  300 mm, GE Corporation) preequilibrated with 50 mM KCl, 0.1 mM EGTA, 10 mM Tris-HCl pH 7.5, 10% glycerol, and 1 mM DTT. The proteins were eluted with the

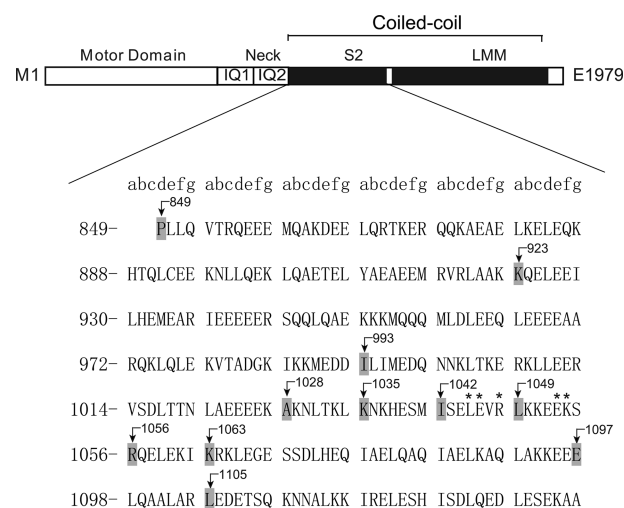


**Figure 1.** Diagram of SmM and the sequence of the S2 coiled-coil. The amino acid residues with arrows in the sequence of the S2 coiled-coil indicate the points of SmM truncation. The positions of each amino acid residue in the coiled-coil heptad repeats are indicated by lower case letters a–g in the top line. Asterisks indicate the “coiled-coil trigger sequence” proposed by Kammerer et al.<sup>23</sup> For clarity, the diagram at the top was not drawn to scale.

same solution at a flow rate of 0.3 mL/min and 300  $\mu\text{L}$  fractions were collected. Fractions containing SmM constructs were analyzed by SDS-PAGE (4–15%) and Coomassie Blue staining.

**Preparation of Smooth Muscle Myosin Light Chain Kinase (MLCK).** cDNA of chicken smooth muscle MLCK (GenBank no. NM\_205459.2) was reverse transcribed from chicken gizzard total RNA using AccuScript Reverse Transcriptase (Stratagene), amplified by Pfu-Ultra (Stratagene) with following primers: 5'-ACTAGGATCCCAAATGGACTTCCGAGCAAAC (underlined, BamHI site) and 5'-ACGTCTC-GAGCCTTGTTTCATTCTTCCTC (underlined, XhoI site), and subcloned into the BamHI site and XhoI site of pFastBacHTb (Life Technology). The recombinant baculovirus encoding MLCK was prepared using A Bac-To-Bac kit (Life Technology) and used to infect Sf9 insect cells. The Sf9-expressed MLCK was purified by Ni-NTA agarose (Qiagen) according to the standard protocol. The purified MLCK was dialyzed against 25 mM Tris-HCl pH 7.5, 30 mM KCl, 0.5 mM DTT, and 1 mM EGTA before being aliquoted in small volumes, quickly frozen, and stored in  $-80^{\circ}\text{C}$ .

**ATPase Assay.** The actin-activated ATPase activity of SmM was assayed at  $25^{\circ}\text{C}$  using an ATP regeneration system as described.<sup>17</sup> Unless otherwise indicated, the actin-activated ATPase assays for unphosphorylated conditions were conducted in a solution containing  $\sim 3 \mu\text{M}$  SmM head, 0.3 mM ATP, 32 mM KCl, 30 mM Tris-HCl pH 7.5, 1 mM  $\text{MgCl}_2$ , 1 mM EGTA, 20 U/mL pyruvate kinase, 2.5 mM phosphoenolpyruvate, and varying concentrations of actin. The actin-activated ATPase assays under phosphorylated conditions were conducted similarly, except that the  $\sim 0.3 \mu\text{M}$  SmM head was used and 1 mM EGTA was replaced by 0.2 mM  $\text{CaCl}_2$ , 15  $\mu\text{g}/\text{mL}$  MLCK, and 1.0  $\mu\text{M}$  CaM. The time course of ATP hydrolysis was measured up to 120 min.  $\text{Ca}^{2+}$ -ATPase activity of SmM was measured at  $25^{\circ}\text{C}$  in 10 mM  $\text{CaCl}_2$ , 0.5 M KCl, 30 mM Tris-HCl, pH 8.5, and 0.25 mg/mL BSA.  $\text{K}^+$ (EDTA)-ATPase activity was measured similarly as  $\text{Ca}^{2+}$ -ATPase activity except that 10 mM  $\text{CaCl}_2$  was replaced by 10 mM EDTA. The

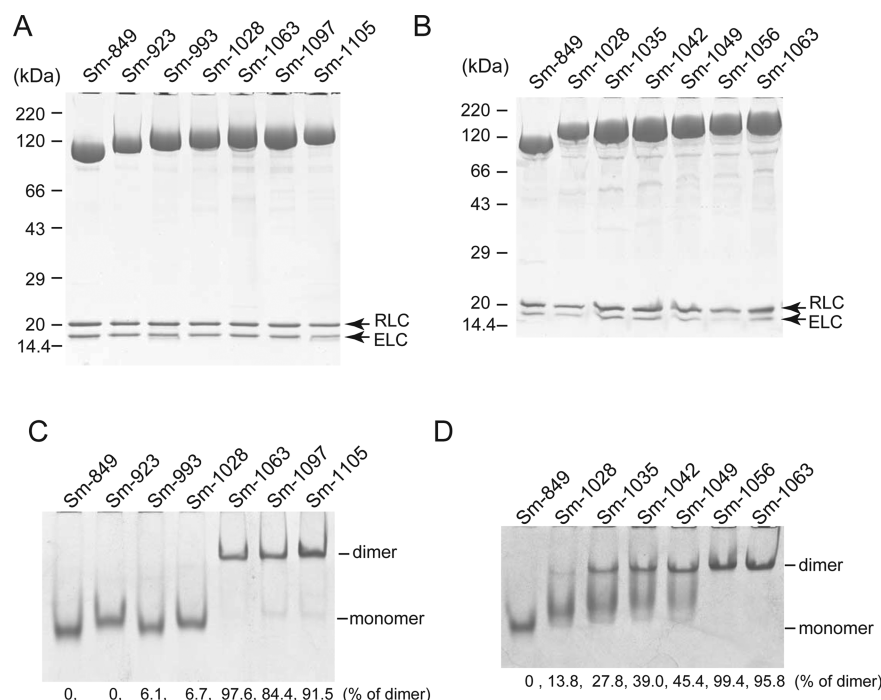


**Figure 2.** Truncations of the S2 coiled-coil rod reveals the critical region for forming stable double-headed structures of SmM. Purified SmM constructs were analyzed by SDS-PAGE (4–20%) and native PAGE (5%). (A and B) SDS-PAGE shows the components of the purified SmM constructs. Arrows indicate the RLC and the ELC copurified with SmM heavy chain. (C and D) Native PAGE shows the dimerization (single-headed structure versus double-headed structure) of the purified SmM constructs. The number below the gels indicates the estimated percentage of double-headed structure using densitometry.

liberated phosphate was determined by the malachite green method.<sup>18</sup>

**Urea/Glycerol Gel Electrophoresis.** Phosphorylation of the RLC was detected by urea/glycerol gel electrophoresis as described<sup>19</sup> with minor modification. Briefly, the SmM constructs (~2  $\mu$ M head) were incubated with MLCK (15  $\mu$ g/mL) in a solution containing 32 mM KCl, 30 mM Tris-HCl pH 7.5, 1 mM MgCl<sub>2</sub>, 1 mM DTT, 0.3 mM ATP, 2.0  $\mu$ M CaM, and 0.2 mM CaCl<sub>2</sub> at 25 °C. At the indicated times, SmM samples were precipitated by addition of 100% TCA to a final concentration of 5% and collected by centrifugation. The precipitated proteins were dissolved in an appropriate volume of sample solution (8.0 M urea, 10 mM dithiothreitol, 0.004% bromophenol blue) to ensure the RLC concentration was about 0.2 mg/mL, and a small amount of 1 M Tris base was added to ensure proper pH as indicated by the blue color of sample solution. The urea-solubilized samples were electrophoresed at 300 V for 2 h in a 1.0-mm polyacrylamide slab gel containing 10% acrylamide, 0.5% bisacrylamide, 40% glycerol, 16 mM Tris base, and 137.5 mM glycine. Prior to loading samples, pre-electrophoresis at 300 V for 1 h was performed. The reservoir buffer contained 16 mM Tris base, 137.5 mM glycine, and 0.4% 2-mercaptoethanol. The protein bands were visualized by Coomassie Brilliant Blue R250 staining.

**Protease Treatment of Sm-849.** Papain (5 mg/mL) was preactivated with 20 mM DTT, 30 mM Tris-HCl (pH 8.0), and 1 mM EDTA at 37 °C for 45 min before use. About 2  $\mu$ M of Sm-849 was incubated with activated papain (0–20  $\mu$ g/mL) or SAP-V8 (0–10 U/mL) in a solution containing 50 mM KCl, 10 mM Tris-HCl, pH 7.5, 0.1 mM EGTA, 1 mM DTT, and 10% glycerol at 37 °C for 75 min (papain) or 90 min (SAP-V8). The ATPase activity of the protease-treated Sm-849 was measured immediately under the unphosphorylated condition (32 mM

KCl, 30 mM Tris-HCl, pH 7.5, 1 mM MgCl<sub>2</sub>, 1 mM EGTA, 0.3 mM ATP, 0.5 mg/mL BSA, 10  $\mu$ g/mL Leupeptin, and 0 or 80  $\mu$ M actin). To prepare the samples for SDS-PAGE, the papain-digested samples were treated with 10 mM iodoacetic acid to inactivate papain before they were boiled in SDS-PAGE loading buffer. No specific treatment was applied to SAP-V8 treated samples.

**Other Assays.** Metal-shadowed electron microscopy was done as described previously<sup>20</sup> except that the SmM construct samples were diluted with 0.1 M ammonium acetate and 30% glycerol. Native PAGE was performed to determine the dimerization of the SmM constructs as described,<sup>21</sup> except that 5% acrylamide–bisacrylamide (29:1) was used and MgATP was omitted from the solution and gel.

## RESULTS

**Identification of the Key Segment in the Coiled-Coil for Stable Double-Headed Structures of SmM.** To investigate the phosphorylation-dependent regulation of SmM, we produced a number of SmM constructs by truncating the coiled-coil of the heavy chain (Figure 1). The expressed SmM constructs were purified by anti-FLAG affinity chromatography. SDS-PAGE showed that the purified SmM constructs had molecular masses as expected from their amino acid sequence and associated stoichiometrically with ELC and RLC (Figure S1).

It is well-established that SmM molecules form a double-headed structure via the C-terminal coiled-coil of the heavy chain, and that SmM constructs without coiled-coil, i.e., S1 (such as Sm-849 here), are single-headed.<sup>8,13,22</sup> Previous work showed that the coiled-coil between residues 1025 and 1109 (heptads 25 and 37) are essential for the formation of a double-headed structure.<sup>13,22</sup> In those studies, the distinction between



a single-headed and a double-headed structure was based on a single criterion, i.e., the migration rate of SmM in native PAGE. However, the effect of electrophoresis on the stability of the double-headed structure of SmM is not known. Here, we investigated the dimerization of SmM using three complementary approaches.

First, we compared the migration rate of SmM truncated constructs in native PAGE. In general agreement with previous studies,<sup>13,22</sup> native PAGE showed two distinct bands for SmM constructs. The slower and faster bands correspond to the dimer (double-headed structure) and to the monomer (single-headed structure) of SmM, respectively (Figure 2C). SmM constructs with a long coiled-coil, such as Sm-1105, -1097, and -1063, migrated more slowly than the SmM constructs with a short coiled-coil, such as Sm-1028, -993, -923, or -849 (Figure 2C). The proportion of dimers (double-headed structures) in each SmM truncated construct was measured by densitometry, and the results are summarized in Table 1. These results suggest that Sm-1105, -1097, and -1063 are mostly dimers and that Sm-1028, -993, -923, and -849 are mostly monomers.

**Table 1. Percentage of the Double-Headed Structure of SmM Constructs**

SmM construct	native PAGE <sup>a</sup>	electron microscopy <sup>b</sup>	size exclusive chromatography <sup>c</sup>
Sm-849	0 (4)	0 (269)	0
Sm-923	0 (3)	8.5 (387)	14.7
Sm-993	4.9 ± 4.3 (4)	46.5 (318)	24.0
Sm-1028	10.7 ± 7.7 (4)	64.1 (222)	68.3
Sm-1063	98.4 ± 2.0 (4)	96.8 (292)	100

<sup>a</sup>Based on native PAGE (Figure 2). The number in parentheses indicates the number of independent experiments. Values are mean ± SD from four independent assays. <sup>b</sup>Based on electron microscopy (Figure 3). The number in parentheses indicates the total number of molecules counted. <sup>c</sup>Based on size exclusive chromatography (Figure 4). For further details see Table S1.

Second, we examined images of the SmM constructs using metal-shadowed electron microscopy (EM). Consistent with the native PAGE results, metal-shadowed EM showed that Sm-1063 and Sm-1097 were mostly double-headed, and Sm-849 was single-headed. Unexpectedly, EM imaging showed that Sm-923, -993, and -1028 were mixtures of single-headed and double-headed molecules (Figure 3). From these images, we estimated that about 8.5% of Sm-923, 46.5% of Sm-993, and 64.1% of Sm-1028 molecules were double-headed (Table 1). One immediate explanation for the discrepancy between native PAGE and EM imaging is that EM imaging might have overestimated the proportion of double-headed molecules versus single-headed molecules. Alternatively, the double-headed structures of Sm-923, -993, and -1028 may have greater stability under the EM conditions than under the native PAGE conditions.

Third, we examined the elution profile of SmM constructs by size-exclusion chromatography in a solution similar to the ATPase assay conditions (Figure 4). The elution fractions were analyzed by SDS-PAGE and Coomassie Blue staining to determine the elution peak of each SmM construct. Since both native PAGE and metal-shadowed EM showed that Sm-849 was single-headed and Sm-1063 was double-headed, we used these two SmM constructs as standards to calibrate the apparent molecular weight (MW) of other constructs. The

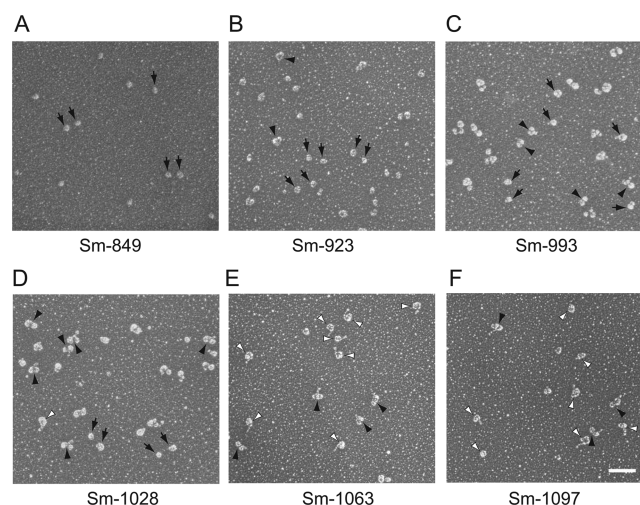


**Figure 3.** Metal-shadowed electron microscopy of SmM constructs. (A) shows that most molecules of Sm-849 are single-headed, (B–D) show that Sm-923, -993, and -1028 are mixtures of single-headed and double-headed molecules, and (E) and (F) show that Sm-1063 and Sm-1097 molecules are double-headed. Black arrow, single-headed molecule; black arrowhead, double-headed molecule in open conformation; white arrowhead, double-headed molecule in closed conformation. The folded, double-headed conformation is similar to the image of folded HMM visualized by negative-staining electron microscopy.<sup>28</sup> Scale bar, 100 nm.

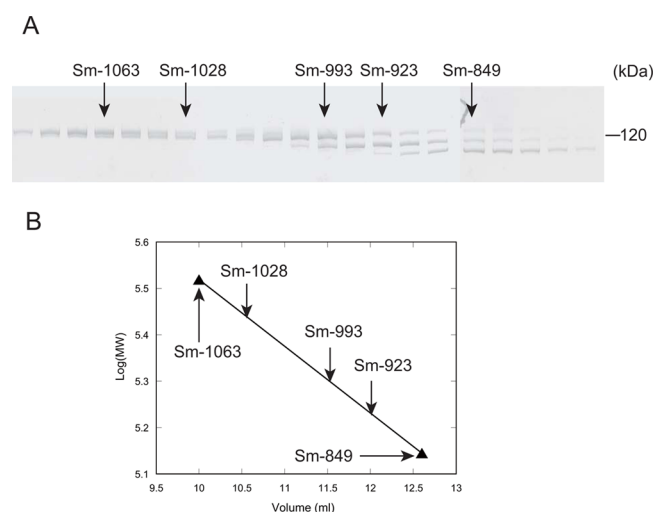


**Figure 4.** Size-exclusion chromatography of SmM constructs. (A) Five purified SmM truncated constructs, i.e., Sm-849, Sm-923, Sm-993, Sm-1028, and Sm-1063, were mixed together and subjected to a Superdex G200 size-exclusion chromatography. The fractions (300  $\mu$ L each) were collected and analyzed by SDS-PAGE (4–15%) and Coomassie Blue staining. The arrows indicate the elution peak of each SmM construct. (B) The apparent molecular weights of Sm-923, -993, and -1028 were calculated using Sm-849 (single-headed) and Sm-1063 (double-headed) as standards based on the elution profile of size-exclusion chromatography. The percentage of the double-headed structures of Sm-923, -993, and -1028 was calculated based on the apparent molecular weight and summarized in Table 1. For details see Table S1.

apparent MW for Sm-923, -993, and -1028 were determined to be 170.3 kDa, 194.4 kDa, and 270.8 kDa, respectively, which are all greater than the MW of corresponding single-headed species but smaller than those of double-headed species (Table

S1), indicating that these three constructs exist as a mixture of single-headed and double-headed molecules. We estimated that the proportions of double-headed molecules were about 15% for Sm-923, 24% for Sm-993, and 68% for Sm-1028 (Table S1 and Table 1). These results were consistent with the observation by metal-shadowed EM (Figure 3) that Sm-923, -993, and -1028 were mixtures of single-headed and double-headed molecules. We reasoned that the double-headed structures of these three SmM constructs were labile and tend to become single-headed under native PAGE conditions (Figure 2C).

In contrast to these labile double-headed structures, Sm-1063, -1097, and -1105 formed more stable double-headed structures (Figure 2C), indicating that the coiled-coil segment between 1028 and 1063 is critical for maintaining a stable double-headed structure. To further define the critical region for stability of the double-headed structure, we created four additional SmM constructs with truncations between residues 1028 and 1063, i.e., Sm-1035, -1042, -1049, and -1056 (Figures 1 and 2B). Native PAGE showed that, similar to Sm-1063, Sm-1056 formed a stable double-headed structure, while all other SmM constructs formed less stable double-headed structures (Figure 2D), indicating that the residues between 1049 and 1056 are essential for double-headed structure stability. For simplicity, we hereafter refer to Sm-1105, -1097, -1063, and -1056 as stable HMM, to Sm-849 as S1, and to the other SmM truncations as unstable HMM.

By analyzing the sequences of the yeast transcriptional activator GCN4 and SmM, Kammerer et al.<sup>23</sup> previously identified a sequence pattern, called the “coiled-coil trigger sequence”, that is absolutely required for the assembly of the GCN4 Leu-zipper. The coiled-coil trigger sequence in SmM is located between residues 1045 and 1054<sup>23</sup> (Figure 1). Our results demonstrated that the coiled-coil trigger sequence is also required for the stable double-headed structure of SmM.

**A Double-Headed Structure Is Essential for SmM Activation by Phosphorylation.** We found that the  $\text{Ca}^{2+}$ -ATPase and  $\text{K}^+(\text{EDTA})$ -ATPase activities of Sm-849 and Sm-923 were similar to those of Sm-1063 and Sm-1097 (Table 2), indicating that truncation of the coiled-coil did not substantially change the motor domain's ATPase activity *per se*.

**Table 2.  $\text{Ca}^{2+}$ - and  $\text{K}^+(\text{EDTA})$ -ATPase Activity ( $\text{s}^{-1} \text{ head}^{-1}$ ) of SmM Constructs<sup>a</sup>**

	$\text{Ca}^{2+}$ -ATPase activity	$\text{K}^+(\text{EDTA})$ -ATPase activity
Sm-849	$0.61 \pm 0.02$	$1.35 \pm 0.11$
Sm-923	$0.66 \pm 0.06$	$1.56 \pm 0.08$
Sm-1063	$0.70 \pm 0.12$	$1.87 \pm 0.04$
Sm-1097	$0.66 \pm 0.09$	$1.74 \pm 0.11$

<sup>a</sup>The  $\text{K}^+(\text{EDTA})$ -ATPase activity was measured similarly to  $\text{Ca}^{2+}$ -ATPase activity, except using 10 mM EDTA instead of 10 mM  $\text{CaCl}_2$ . The liberated phosphate was determined by the malachite green method. Values are mean  $\pm$  SD from three independent assays.

To assess the effect of coiled-coil truncation on the phosphorylation-dependent regulation, we measured the actin-activated ATPase activity of SmM constructs in the phosphorylated and the unphosphorylated conditions. As shown in Figure 5, the actin-activated ATPase activity of stable HMM (Sm-1063, Sm-1097, and Sm-1105) was well regulated by phosphorylation (Figure 5E–G), while that of Sm-849 was not (Figure 5A). Notably, the actin-activated ATPase activity of

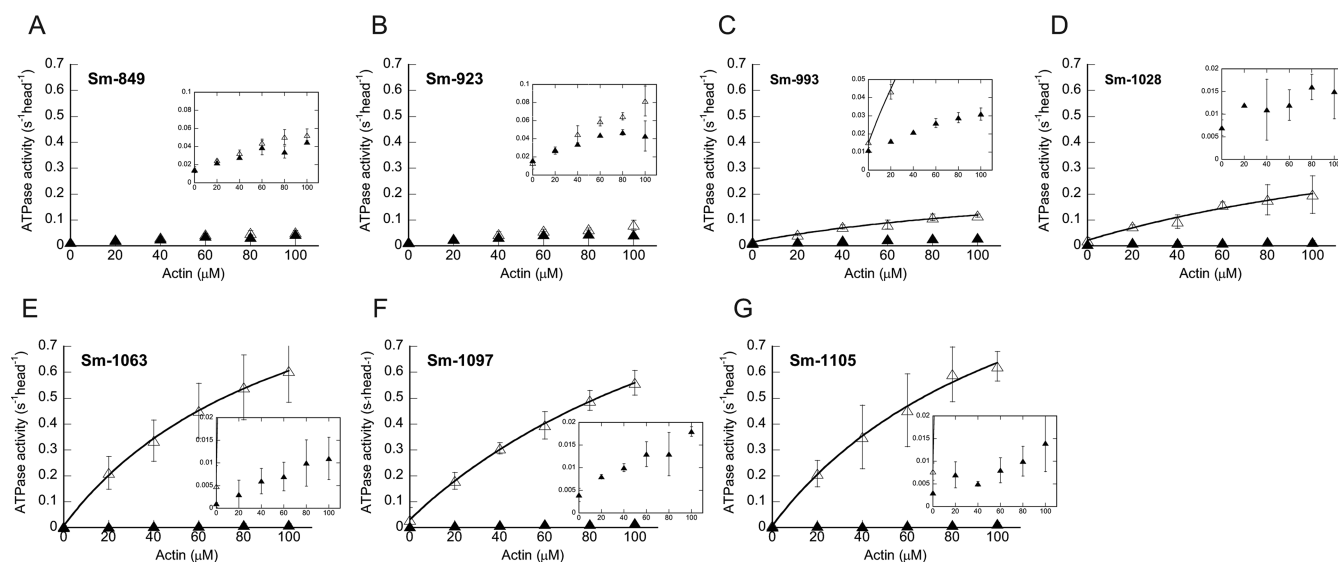
Sm-849, regardless of phosphorylation, was much lower than that of phosphorylated stable HMM, although higher than that of the unphosphorylated stable HMM (Figure 5A). Compared to stable HMM, the actin-activated ATPase activities of unstable HMM were more suppressed when unphosphorylated and partially activated by phosphorylation (Figure 5B–D).

Figure 6 summarizes the effects of coiled-coil length on the actin-activated ATPase activity of SmM in the phosphorylated and the unphosphorylated state. In the unphosphorylated state, the actin-activated activity of SmM decreased as the coiled-coil length increased (Figure 6). When the coiled-coil was longer than 179 aa (i.e., for Sm-1028, -1063, -1097, and -1105), the actin-activated ATPase activity reached the minimum in the unphosphorylated state. Together with the findings that Sm-1028 formed a labile double-headed structure and that Sm-1063, -1097, and -1105 formed stable double-headed structures (Figures 2–4), these results indicate that double-headed structure is essential for full inhibition of unphosphorylated SmM.

On the other hand, in the phosphorylated state, the actin-activated activity of SmM increased as the coiled-coil increased (Figure 6A). When the coiled-coil was longer than 214 aa (i.e., for Sm-1063, -1097, and -1105), the actin-activated ATPase activity reached the maximum for the phosphorylated state. Since Sm-1063, -1097, and -1105 form stable double-headed structures (Figure 2), we propose that a stable double-headed structure is essential for full activation of the phosphorylated SmM.

To determine whether the low actin-activated ATPase activity of Sm-849 in phosphorylated conditions could be due to insufficient phosphorylation of the RLC, we compared the level of phosphorylation of Sm-849 and Sm-1063 under the same ATPase assay conditions. Urea/glycerol gel electrophoresis showed that, similar to that of Sm-1063, the RLC of Sm-849 was fully phosphorylated within 10 s (data not shown). Therefore, the low actin-activated ATPase activity of Sm-849 under the phosphorylation conditions was not due to insufficient phosphorylation of the RLC.

**Protease Treatment Enhances the Activity of S1.** The ATPase activity of SmM (Figure 5) increased almost linearly without saturation under our assay conditions, i.e., in the presence of 30 mM KCl, prevented us from obtaining  $V_{\text{max}}$ . It is known that the affinity of SmM for actin increases with decreasing ionic strength. In an attempt to obtain the  $V_{\text{max}}$  for the actin-activated ATPase activity of Sm-849 (S1) and Sm-1063 (a stable HMM), we also performed the ATPase assays in the presence of 10 mM KCl, the lowest ionic strength permitted in our ATPase assays, and at an actin concentration up to 200  $\mu\text{M}$  (Figure S2). Under these conditions, the ATPase activity of Sm-1063 was well regulated by phosphorylation, with a  $V_{\text{max}}$  of  $0.036 \text{ s}^{-1}$  in the unphosphorylated state and  $2.935 \text{ s}^{-1}$  in the phosphorylated state. In contrast, the ATPase activity of Sm-849 was not regulated by phosphorylation, with a  $V_{\text{max}}$  of  $0.268 \text{ s}^{-1}$  in the unphosphorylated state and  $0.282 \text{ s}^{-1}$  in the phosphorylated state. The  $V_{\text{max}}$  of unphosphorylated Sm-849 was about 7 times higher than that of unphosphorylated Sm-1063, indicating that a stable double-headed structure is essential for full inhibition in the unphosphorylation state. On the other hand, in the phosphorylated state, the  $V_{\text{max}}$  of Sm-849 was only about 10% of that of Sm-1063, indicating that full activation by phosphorylation also requires a stable double-headed structure. It should be noted that the highest actin concentration used (200  $\mu\text{M}$ ) was far below the  $K_m$  of Sm-849



**Figure 5.** Actin-activated ATPase activity of SmM constructs. The actin-activated ATPase activity of SmM was assayed in either unphosphorylated or phosphorylated conditions. (A–G) Sm-849, -923, -993, -1028, -1063, -1097, and Sm-1105, respectively. The insets show the ATPase activities on a shorter scale. For the actin-activated ATPase activity of Sm-993, -1028, -1063, -1097, and -1105 in the phosphorylated conditions, curves are the least-squares fits of the data points based upon the equation:  $V = (V_{\max} \times [\text{actin}]) / (K_{\text{actin}} + [\text{actin}]) + V_0$ , where  $V_{\max}$  is the maximal activity;  $K_{\text{actin}}$  is the apparent dissociation constant for actin; and  $V_0$  is the activity in the absence of actin. Filled symbols are the unphosphorylated conditions; open symbols, the phosphorylated conditions. All data are the average of at least two independent assays.

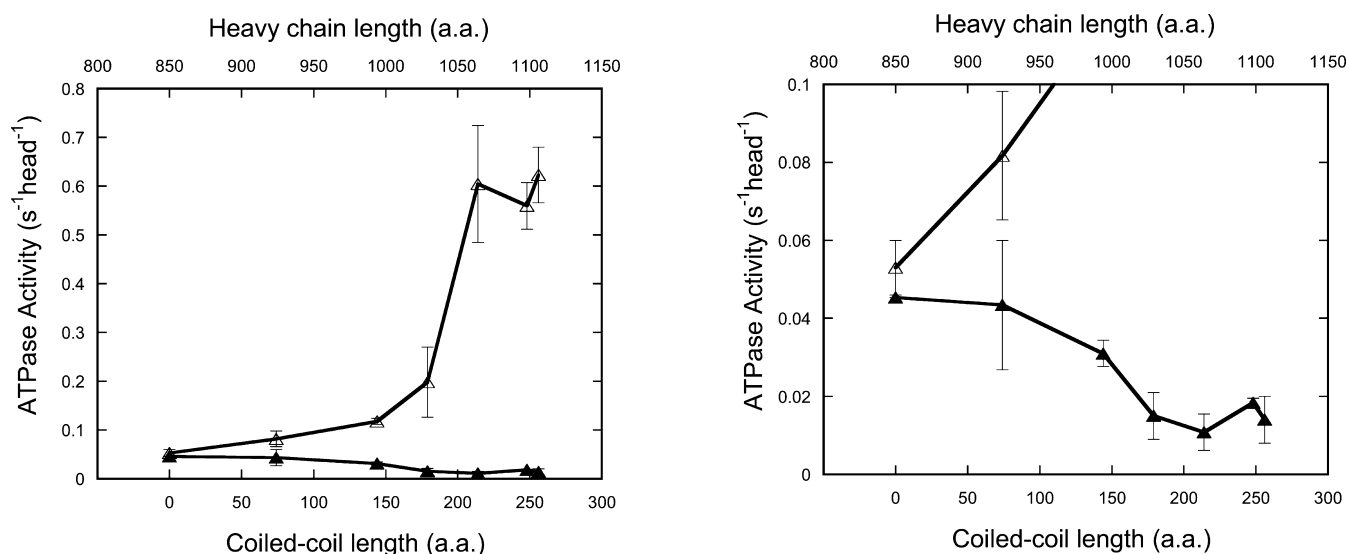


**Figure 6.** Relationship between the actin-activated ATPase activity and coiled-coil length. The ATPase activities of SmM constructs in the presence of 100  $\mu\text{M}$  actin (data from Figure 5) are plotted against the length of the coiled-coil, which are 0, 74, 144, 179, 214, 248, and 256 amino acids for Sm-849, -923, -993, -1028, -1063, -1097, and -1105, respectively. Filled symbols are the unphosphorylated conditions; open symbols, the phosphorylated conditions. For clarity, the ATPase activities were plotted at two scales, a regular scale (left), and a shorter scale (right). Note: Since the ATPase activity of SmM (Figure 5) increased almost linearly without saturation under the assay conditions, i.e., 0–100  $\mu\text{M}$  actin, no attempts were made to obtain  $V_{\max}$  and  $K_{\text{actin}}$ , and therefore the regulation of SmM was based on actin-activated ATPase activity in the presence of 100  $\mu\text{M}$  actin, instead of  $V_{\max}$ .

( $\sim 450 \mu\text{M}$ ), and thus the calculated  $V_{\max}$  values for Sm-849 are not accurate. Nevertheless, the actin-activated ATPase activities of Sm-849 in all actin concentrations tested were higher than these of unphosphorylated Sm-1063, but lower than these of phosphorylated Sm-1063.

Notably, the actin-activated ATPase activity of recombinant S1, i.e., Sm-849, was also lower than the reported values of proteolytic S1.<sup>8,10</sup> One possible explanation is the presence of the internal nicks in the latter. To test this possibility, we treated Sm-849 with two proteases, i.e., papain or *Staph-*

*tylococcus aureus* V8 protease (SAP-V8), and measured the ATPase activity after the treatment. As shown in Figure 7A, papain digestion markedly enhanced the actin-activated ATPase activity of Sm-849. SDS-PAGE analysis showed that the increase of ATPase activity was accompanied by cleavage of the heavy chain, ELC and RLC (Figure 7A,B). Similar results were obtained for the SAP-V8 treated Sm-849, except that in these cases only the heavy chain was cleaved (Figure 7C,D). These results suggest that the relatively high ATPase activity of proteolytically prepared S1 in the previous studies<sup>8–11</sup> was



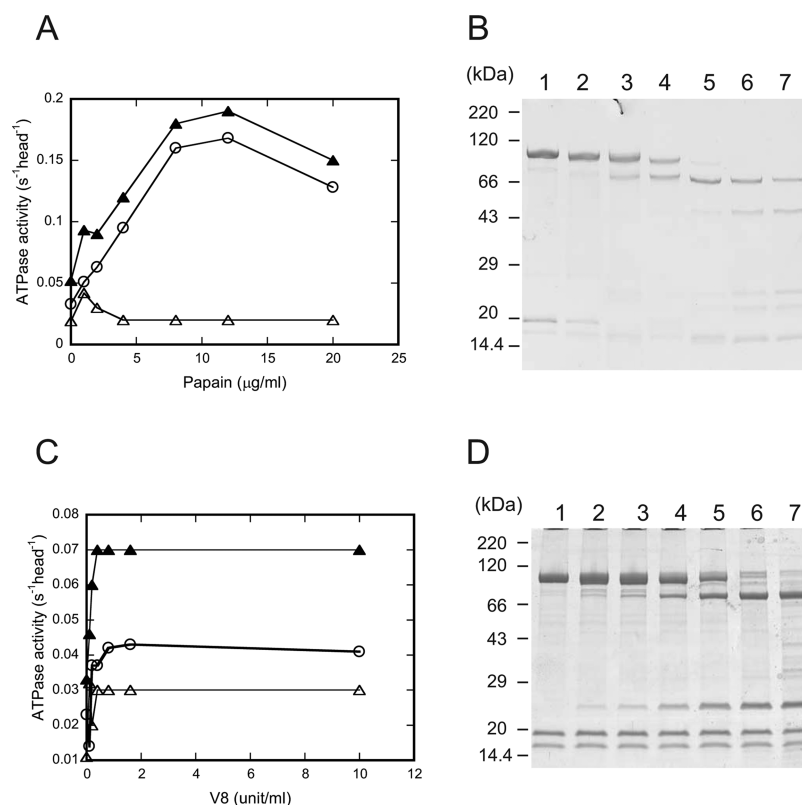


**Figure 7.** Effects of protease treatment on the ATPase activity of Sm-849. (A,B) Purified Sm-849 was digested with various concentrations of papain (0–20 μg/mL) and immediately subjected to ATPase assays (A) and SDS-PAGE analysis (B). (C, D) Purified Sm-849 was digested with various concentrations of SAP-V8 protease (0–10 unit/ml) and immediately subjected to ATPase assays (C) and SDS-PAGE analysis (D). Open triangles are in the absence of actin; closed triangles, in the presence of 80 μM actin; open circles are the actin-activated ATPase activity.

likely due to internal cleavages of the heavy chain and/or light chains by protease.

## DISCUSSION

The prevailing model for the regulation of SmM by phosphorylation is that the inhibited state of unphosphorylated SmM is dependent upon interactions between the two heads and between the heads and the coiled-coil tail, and that phosphorylation disrupts those interactions, thus reversing the inhibition and stimulating motor activity to the maximal value.<sup>8–11</sup> One assumption of this model is that single-headed SmM, such as S1, has the same actin-activated ATPase activity as phosphorylated double-headed SmM. Our current studies indicate that this assumption is incorrect. We found that the actin-activated ATPase activity of S1, regardless of phosphorylation, was about 10 times lower than that of the phosphorylated double-headed HMM. We also demonstrated that the relatively high ATPase activity of proteolytically prepared S1 in earlier studies<sup>8–11</sup> was likely due to unintended internal cleavages of the heavy chain and/or the light chains. Therefore, we propose that single-headed SmM, such as S1, regardless of phosphorylation, is not fully active.

Recently, Decarreau et al.<sup>24</sup> generated a single-headed SmM construct, MDE (a truncated SmM S1 containing only the motor domain and ELC). The  $V_{\max}$  of the actin-activated ATPase activity of MDE (0.74 s<sup>-1</sup>)<sup>24</sup> at 37 °C was found to be about one-eighth of that of the phosphorylated double-headed HMM (~6 s<sup>-1</sup>, estimated from another study)<sup>22</sup> under a similar assay condition, consistent with our proposal that single-headed SmM is not fully active.

We found that only those SmM constructs capable of forming stable double-headed structures were able to be fully activated when the RLC was phosphorylated. Shortening the coiled-coil destabilized the double-headed structure and dampened the actin-activated ATPase activity of phosphorylated SmM, suggesting that the head–head cooperation is essential for the full activation of SmM by phosphorylation.

Although smooth muscle S1 is not fully active, neither is it fully inhibited. Our results show that the actin-activated ATPase activity of S1 was substantially higher than that of unphosphorylated double-headed SmM. This result is consistent with the prevailing view on the structure of inhibited SmM, which is formed by the folding of two heads such that they interact with each other and with the coiled-coil.<sup>2</sup> Thus, proper interactions between the head and the tail and/or between the two heads are essential for the inhibition, and short of such interactions the head is rendered partially active. Decreasing the length of the SmM coiled-coil decreases the above-mentioned interactions, thus also weakens the inhibition and elevates the ATPase activity.

Cremo and associates reported that single-headed SmM prepared by limited protease-treatment is as active as double-headed SmM under phosphorylated conditions, indicating a fully activated state.<sup>25</sup> However, Konishi et al.<sup>14</sup> found that, similar to S1, recombinant single-headed HMM is much less active than recombinant double-headed HMM in phosphorylated forms, although it is more active than unphosphorylated double-headed HMM. The discrepancy between these two studies may be explained by the presence of unintended

cleavages of the heavy chain in the proteolytic single-headed SmM but not in the recombinant single-headed HMM.

Based on all the above findings, we propose that the inhibition of unphosphorylated SmM involves specific head–tail interactions and/or head–head interactions, and that the activation of SmM by phosphorylation requires optimal cooperation between the two heads. Thus, disruption of the head–tail interaction and/or the head–head interaction in unphosphorylated SmM will compromise the inhibition and elevate the ATPase activity. On the other hand, disruption of the cooperation between the two heads of the phosphorylated SmM will decrease the ATPase activity. These scenarios are consistent with the observation that most mutant and truncated constructs of SmM, which have lost their normal regulation, also exhibit elevated ATPase activity in the unphosphorylated state, whereas their ATPase activity in the phosphorylated state is attenuated relative to wild type.

On the basis of all the above findings, a new model for SmM regulation emerges in which both the inhibition of the unphosphorylated SmM and the activation of phosphorylated SmM require optimal cooperation between the two heads. Disruption of the head–tail interaction and/or the head–head interaction in the unphosphorylated state will compromise the inhibition and elevate the ATPase activity. Likewise, disruption of the cooperation between the two heads of the phosphorylated SmM will also decrease the ATPase activity. These scenarios are consistent with the observation thus far that mutant and truncated constructs of SmM having lost normal regulation have an elevated ATPase activity in the unphosphorylated state and attenuated ATPase activity in the phosphorylated state relative to the wild type.

One example is the so-called “asymmetric HMM”. Three groups have independently investigated the regulation of HMM variants containing one intact head and one truncated head.<sup>14,20,26</sup> Although the structures of the asymmetric HMM in these studies are not the same (and the conclusions are different), none of these asymmetric HMM are as well regulated as double-headed HMM (Table S2). Another common feature is that all these asymmetric HMM display lower ATPase activity than double-headed HMM in the phosphorylated state. The latter results have not been adequately addressed, and they contradict the prevailing model. In light of our proposed model, further investigations and/or reinterpretation of those earlier studies is warranted. According to our proposed model, the absence of head–head cooperation in these asymmetric HMM would account for the observed low activity in phosphorylated state compared to wild type.

A final discrepancy remains to be satisfactorily resolved. While Li et al.<sup>20</sup> and Konish et al.<sup>14</sup> showed that, in phosphorylated state, the ratio between the ATPase activities of asymmetric HMM and that of double-headed HMM is between 7% and 16%, Sweeney et al.<sup>26</sup> reported the ratio to be between 40% and 60% (Table S2). In the former two studies, the enzymatic activity of the asymmetric HMM was similar to that of S1, consistent with what one would expect for a molecule having single globular head attached to an  $\alpha$ -helical tail. In the latter study, the enzymatic activity of the asymmetric HMM is significantly higher than that of S1, suggesting that the coiled-coil somehow stimulates the activity of the single head. Although the reason for this inconsistency remains to be resolved, the results from the former two studies are consistent with our proposed model for SmM regulation.

Our proposed model of cooperation between the two heads of myosin in the phosphorylated state is not unique to SmM. It has also been shown to exist in nonmuscle myosin II such as *Dictyostelium* myosin II<sup>5</sup> and chicken nonmuscle myosin IIB.<sup>27</sup> In both cases, the single-headed constructs have about 2-fold lower activity per head than the double-headed constructs.<sup>5,27</sup> The nature of cooperation between the two heads of the phosphorylated SmM and nonmuscle myosin II is far from clear and deserves further investigation.

## ■ ASSOCIATED CONTENT

### ■ Supporting Information

Relative amount of the single-headed and double-headed forms of SmM constructs estimated from size-exclusive chromatography (Table S1), summary of the actin-activated ATPase activity of asymmetric single-headed SmM (Table S2), ratios of RLC versus the heavy chain and ELC versus the heavy chain of SmM truncated constructs (Figure S1), and the actin-activated ATPase activities of Sm-849 and Sm-1063 in low salt conditions (Figure S2). This material is available free of charge via the Internet at <http://pubs.acs.org>.

## ■ AUTHOR INFORMATION

### Corresponding Author

\*Tel: 8610-64806015; E-mail: [lixd@ioz.ac.cn](mailto:lixd@ioz.ac.cn).

### Funding

This work was supported by the National Basic Research Program of China (No. 2013CB932802 and No. 2012CB114102), the National Natural Science Foundation of China (No. 31171367 and 31071973), and the State Key Laboratory of Integrated Management of Pest Insects and Rodents (No. ChineseIPM1102).

### Notes

The authors declare no competing financial interest.

## ■ ACKNOWLEDGMENTS

We thank Ms. Dan Luo for subcloning of SmM constructs. We thank Dr. Mei Shen and Ms. Weixiao Liu for setting up size-exclusion chromatography. We thank Dr. Paul Odgren (University of Massachusetts Medical School) for reading the manuscript.

## ■ ABBREVIATIONS

SmM, smooth muscle myosin; HMM, heavy meromyosin; S1, subfragment 1 of smooth muscle myosin; CaM, calmodulin; RLC, regulatory light chain; ELC, essential light chain; SAP-V8, *Staphylococcus aureus* V8 protease; PAGE, polyacrylamide gel electrophoresis; DTT, dithiothreitol; EGTA, ethylene glycol-bis(2-aminoethyl ether)-N,N,N',N'-tetraacetic acid

## ■ REFERENCES

- (1) Kamm, K. E., and Stull, J. T. (1989) Regulation of smooth muscle contractile elements by second messengers. *Annu. Rev. Physiol.* 51, 299–313.
- (2) Lowey, S., and Trybus, K. M. (2010) Common structural motifs for the regulation of divergent class II myosins. *J. Biol. Chem.* 285, 16403–16407.
- (3) Margossian, S. S., and Lowey, S. (1973) Substructure of the myosin molecule. IV. Interactions of myosin and its subfragments with adenosine triphosphate and F-actin. *J. Mol. Biol.* 74, 313–330.
- (4) Mockrin, S. C., and Spudich, J. A. (1976) Calcium control of actin-activated myosin adenosine triphosphatase from *Dictyostelium discoideum*. *Proc. Natl. Acad. Sci. U. S. A.* 73, 2321–2325.



- (5) Ito, K., Liu, X., Katayama, E., and Uyeda, T. Q. (1999) Cooperativity between two heads of dictyostelium myosin II in in vitro motility and ATP hydrolysis. *Biophys. J.* 76, 985–992.
- (6) Manstein, D. J., Ruppel, K. M., and Spudich, J. A. (1989) Expression and characterization of a functional myosin head fragment in *Dictyostelium discoideum*. *Science* 246, 656–658.
- (7) Sweeney, H. L. (1998) Regulation and tuning of smooth muscle myosin. *Am. J. Respir. Crit. Care Med.* 158, S95–99.
- (8) Ikebe, M., and Hartshorne, D. J. (1985) Proteolysis of smooth muscle myosin by *Staphylococcus aureus* protease: preparation of heavy meromyosin and subfragment 1 with intact 20 000-dalton light chains. *Biochemistry* 24, 2380–2387.
- (9) Marston, S. B., and Taylor, E. W. (1980) Comparison of the myosin and actomyosin ATPase mechanisms of the four types of vertebrate muscles. *J. Mol. Biol.* 139, 573–600.
- (10) Greene, L. E., Sellers, J. R., Eisenberg, E., and Adelstein, R. S. (1983) Binding of gizzard smooth muscle myosin subfragment 1 to actin in the presence and absence of adenosine 5'-triphosphate. *Biochemistry* 22, 530–535.
- (11) Taylor, E. W. (1977) Transient phase of adenosine triphosphate hydrolysis by myosin, heavy meromyosin, and subfragment 1. *Biochemistry* 16, 732–739.
- (12) Ikebe, M., Mitra, S., and Hartshorne, D. J. (1993) Cleavage at site A, Glu-642 to Ser-643, of the gizzard myosin heavy chain decreases affinity for actin. *J. Biol. Chem.* 268, 25948–25951.
- (13) Sata, M., Matsuura, M., and Ikebe, M. (1996) Characterization of the motor and enzymatic properties of smooth muscle long S1 and short HMM: role of the two-headed structure on the activity and regulation of the myosin motor. *Biochemistry* 35, 11113–11118.
- (14) Konishi, K., Kojima, S., Katoh, T., Yazawa, M., Kato, K., Fujiwara, K., and Onishi, H. (2001) Two new modes of smooth muscle myosin regulation by the interaction between the two regulatory light chains, and by the S2 domain. *J. Biochem.* 129, 365–372.
- (15) Lu, Z., Shen, M., Cao, Y., Zhang, H. M., Yao, L. L., and Li, X. D. (2012) Calmodulin bound to the first IQ motif is responsible for calcium-dependent regulation of myosin 5a. *J. Biol. Chem.* 287, 16530–16540.
- (16) Li, X. D., Mabuchi, K., Ikebe, R., and Ikebe, M. (2004) Ca<sup>2+</sup>-induced activation of ATPase activity of myosin Va is accompanied with a large conformational change. *Biochem. Biophys. Res. Commun.* 315, 538–545.
- (17) Li, X. D., Jung, H. S., Wang, Q., Ikebe, R., Craig, R., and Ikebe, M. (2008) The globular tail domain puts on the brake to stop the ATPase cycle of myosin Va. *Proc. Natl. Acad. Sci. U. S. A.* 105, 1140–1145.
- (18) Kodama, T., Fukui, K., and Kometani, K. (1986) The initial phosphate burst in ATP hydrolysis by myosin and subfragment-1 as studied by a modified malachite green method for determination of inorganic phosphate. *J. Biochem.* 99, 1465–1472.
- (19) Persechini, A., Kamm, K. E., and Stull, J. T. (1986) Different phosphorylated forms of myosin in contracting tracheal smooth muscle. *J. Biol. Chem.* 261, 6293–6299.
- (20) Li, X. D., Saito, J., Ikebe, R., Mabuchi, K., and Ikebe, M. (2000) The interaction between the regulatory light chain domains on two heads is critical for regulation of smooth muscle myosin. *Biochemistry* 39, 2254–2260.
- (21) Trybus, K. M., and Lowey, S. (1985) Mechanism of smooth muscle myosin phosphorylation. *J. Biol. Chem.* 260, 15988–15995.
- (22) Trybus, K. M., Freyzon, Y., Faust, L. Z., and Sweeney, H. L. (1997) Spare the rod, spoil the regulation: necessity for a myosin rod. *Proc. Natl. Acad. Sci. U. S. A.* 94, 48–52.
- (23) Kammerer, R. A., Schulthess, T., Landwehr, R., Lustig, A., Engel, J., Aebi, U., and Steinmetz, M. O. (1998) An autonomous folding unit mediates the assembly of two-stranded coiled coils. *Proc. Natl. Acad. Sci. U. S. A.* 95, 13419–13424.
- (24) Decarreau, J. A., James, N. G., Chrin, L. R., and Berger, C. L. (2011) Switch I closure simultaneously promotes strong binding to actin and ADP in smooth muscle myosin. *J. Biol. Chem.* 286, 22300–22307.
- (25) Facemyer, K. C., Sellers, J. R., and Cremo, C. R. (1995) Two heads are required for phosphorylation-dependent regulation of smooth muscle myosin. *Biophys. J.* 68, 228S.
- (26) Sweeney, H. L., Chen, L. Q., and Trybus, K. M. (2000) Regulation of asymmetric smooth muscle myosin II molecules. *J. Biol. Chem.* 275, 41273–41277.
- (27) Cremo, C. R., Wang, F., Facemyer, K., and Sellers, J. R. (2001) Phosphorylation-dependent regulation is absent in a nonmuscle heavy meromyosin construct with one complete head and one head lacking the motor domain. *J. Biol. Chem.* 276, 41465–41472.
- (28) Burgess, S. A., Yu, S., Walker, M. L., Hawkins, R. J., Chalovich, J. M., and Knight, P. J. (2007) Structures of smooth muscle Myosin and heavy meromyosin in the folded, shutdown state. *J. Mol. Biol.* 372, 1165–1178.